Experimental Procedures

Chemicals. Silver nitrate (≥ 99 %), anhydrous 1, 5-pentanediol (≥ 97 %), poly (vinylpyrrolidone) (PVP; average MW = 55000), 1H,1H,2H,2H-perfluorodecanethiol (PFDT, ≥ 97 %), zinc nitrate hexahydrate (98%), 2-methylimidazole (99%), 4-methylbenzenethiol (4MBT, ≥ 98 %), 2-naphthalenethiol (99%), chloroform, toluene, decane (anhydrous, ≥ 99 %), were purchased from Sigma Aldrich; copper (II) chloride (≥ 98 %) was from Alfa Assar; ethanol (ACS, ISO, Reag. Ph. Eur) was from EMSURE®. All chemicals were used without further purification. Milli-Q water (> 18.0 MΩ. cm) was purified with a Sartorius Arium® 611 UV ultrapure water system.

Synthesis and purification of Ag nanocubes. Ag nanocubes were synthesized in high yield via the polyol method according to literature.[1] Copper (II) chloride (8 mg/mL), poly (vinylpyrrolidone) (20 mg/mL) and silver nitrate (20 mg/mL) were separately dissolved in 10 mL 1, 5-pentanediol after repeated sonication and vortex mixing. 35 µL copper (II) chloride solution was subsequently added to the silver nitrate solution. 20 mL of 1,5-pentanediol was added into a 100-mL round bottomed flask and heated to 190 ^{o}C for 10 min. 250 µL poly(vinylpyrrolidone) precursor was added to flask dropwise every 30 s while 500 µL silver nitrate precursor was injected every minute using a quick addition. The addition process continued until the greenish coloration of the mixture faded off.

For the purification of Ag nanocubes, 1, 5-pentanediol was first removed from the mixture through centrifugation and then washed with ethanol. The Ag nanocubes were then dispersed in 10 mL ethanol and 100 mL aqueous poly (vinylpyrrolidone) solution (0.2 g/L). The resulting solution was vacuum filtered using Durapore® polyvinylidene fluoride filter membranes (Millipore) with pore sizes ranging from 5000, 650, 450, and 220 nm, repeated several times for each pore size. The Ag nanocubes were then re-dispersed in ethanol (10 mg/mL) and stored in fridge for further use.

Assembly of Ag nanocubes via Langmiur-blodgett methdod. Si (100) substrates were cleaned prior to assembly of Ag naocubes using oxygen plasma (FEMTO SCIENCE, CUTE-MP/R, 100 W) for 5 min. The surface pressure was zeroed before addition of PVP-caped Ag nanocubes. 700 µl of the ethanolic purified Ag nanocubes was dispersed in 1050 µl of chloroform and then added carefully to the surface of the water in the Langmiur-Bblodgett trough (KSV NIMA, KN1002). The surface pressure can be tuned by moving the mechanical barrier of the machine. Surface pressure of 4, 8, 10, 12, 14, 16, 18 mN/ m were performed, and the pull rates and compression rate were fixed at 2 mm/ s.

1H,1H,2H,2H-perfluorodecanethiol (PFDT) functionalization of Ag nanocubes. The removal of surfactant from Ag nanocubes surface was done by functionalizing the assembled Ag nanocubes with PFDT. The assembled Ag nanocube array was immersed in 5 mM of PFDT methanolic solution for at least 15 hours.

Growth of ZIF-8 film on PFDT-capped Ag nanocubes array. ZIF-8 film was grown on the nanocubes array using a procedure reported from literature.[2] 2 ml of methanolic $Zn(NO_3)_2$ (25 mM) was added to 2 ml of methanolic 2-methylimidazole (mIM; 50 mM) and mixed quickly for 5 s. For one growth cycle, the PFDT-capped Ag nanocubes substrate was immersed in the solution for 40 minutes, and then washed with copious amount of methanol and dried with nitrogen gas several times to remove excess ZIF-8 crystals. The procedure was repeated (1 – 5 times) using fresh $Zn(NO_3)_2$ and 2-methylimidazole solutions to obtain ZIF-8 films of increasing thickness.

Activation of Ag@ZIF substrate. The Ag@ZIF substrates were thermally activated to remove any solvent molecules within its pores by heating the substrate under vacuum at 120ºC for 2 hours. The substrates are used immediately after activation.

Fabrication of Ag film@ZIF. 25-nm Ag film was deposited onto the O_2 plasma-treated Si wafer using a thermal evaporator deposition system from Syskey Technology Corporation (Taiwan) system. The deposition rate was 0.5 Å/s which was monitored using a quartz crystal microbalance. Ag target with 99.99% purity was purchased from Zhongnuo Advanced Material (Beijing) Technology co., Ltd. The Ag film was then functionalized with PFDT and then with 3 layers of ZIF-8 using the same procedures as above.

Fabrication of ZIF only. Silicon substrate was directly immersed in a fresh mixture containing 2 ml of methanolic $Zn(NO_3)_2$ (25 mM) and 2 ml of methanolic 2-methylimidazole (mIM; 50 mM) for 40 minutes, and then washed and dried under nitrogen flow. Additional 2 growth cycles were carried out to achieve ZIF film of similar thickness to Ag@ZIF platform.

Synthesis of Ag@ZIF core-shell. 250 µL of $Zn(NO_3)_2$ (25 mM) was added to a vial of 1.3 mL methanol and stirred at 500 rpm for 5 minutes. 250 µL of methanolic 2-methylimidazole (50 mM) was then added, followed by the immediate addition of 200 µL Ag nanocubes solution (4.7 mg/mL). The mixture was stirred for another 90 minutes at 500 rpm. Excess reagents were removed by centrifugation and the core-shell nanoparticles were then washed twice with methanol and then finally re-dispersed in methanol.

SERS measurement of VOCs and PAH vapors. The activated Ag@ZIF substrate or Ag nanocubes only substrate is incubated together with 200 ul or 0.05 g of solvent/solid at ambient conditions in an enclosed Raman cell printed using Form 1+ stereolithography 3D printer. The SERS detection was performed 10 or 30 mins after incubation of vapor at room temperature (~ 20ºC). Time-dependent investigations were performed using Ag@ZIF-(3) fabricated at Π = 12 mN/m. For VOCs detection, optimized Ag@ZIF-(3) fabricated at Π = 16 mN/m is employed. SERS measurement is performed

using a hyperspectral x-y imaging mode with an acquisition time of 1 s/line or 15 s/line (for toluene and chloroform) and a laser power of 0.5 mW or 0.38 mW respectively, unless otherwise stated.

Characterization. Scanning electron microscope (SEM) and energy-dispersive X-ray spectroscopy (EDS) imaging was performed using JEOL-JSM-7600F microscope. UV-vis spectra were measured with Cary 60 UV-vis spectrometer. Substrate X-ray diffraction patterns were recorded on a Bruker GADDS XRD diffractometer with Cu Ka radiation. SERS measurements were performed using x-y hyperspectral imaging mode of the Ramantouch microspectrometer (Nanophoton Inc., Osaka, Japan) with an excitation wavelength of 532 nm and laser power of 0.5 mW or 0.38 mW. A 50× objective lens (N.A. = 0.55) with 1 s or 15 s acquisition time was used for data collection. All SERS spectra were obtained by averaging the individual SERS spectra within the SERS image.

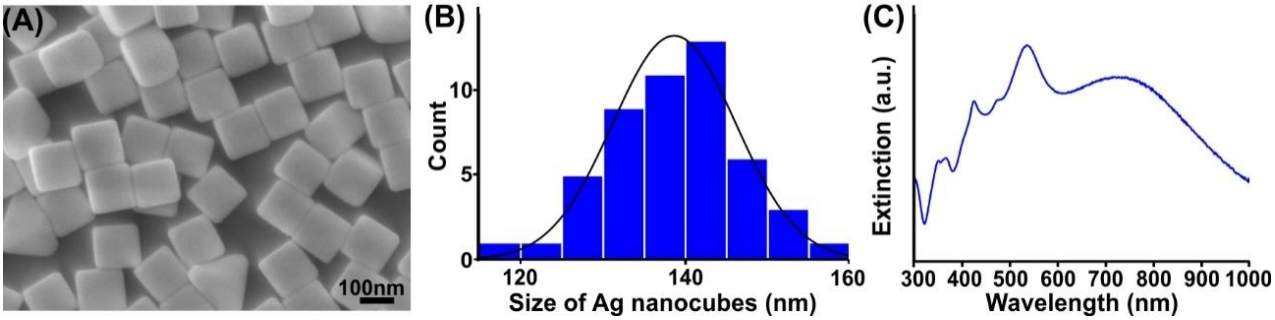

Figure S1. Characterization of as-synthesized PVP-coated Ag nanocubes. (A) SEM image of Ag nanocubes. (B) Size distribution of Ag nanocube edge length. The average edge length is measured at (138 ± 7) nm. (C) UV-vis extinction spectra of the PVP-coated Ag nanocubes colloidal solution in ethanol. The peaks at 353, 400, 505 and 724 nm that can be assigned to octupole (353 nm), quadrupole (400 nm and 505 nm), and dipole resonances (724 nm).[3]

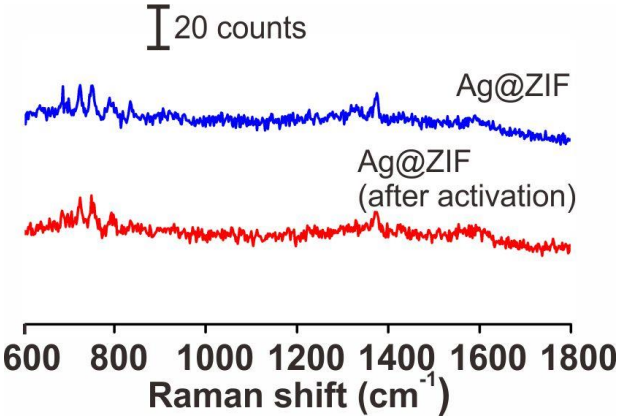

Figure S2. Background spectra of Ag@ZIF platform before (blue) and after (red) thermal activation. The clean background arises due to the functionalization of PFDT ligands onto the Ag nanocubes surface, while the similar vibrational signatures reflect the chemical stability of the platform even after thermal activation.

ZIF provides chemically- and thermally-stable nanoporosity required to preconcentrate various vapor molecules near the Ag surface, while perfluorodecanethiol (PFDT)-capped Ag nanocube offers strong SERS activity with clean signal background for accurate molecular identification.[4]

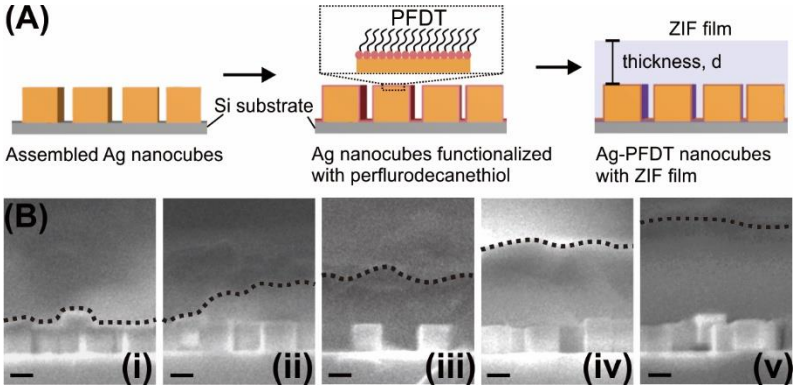

Figure S3. (A) Scheme of thin film formation of ZIF-8 onto assembled Ag nanocubes substrate; Ag nanocubes array are first immersed into PFDT solution (5 mM) for above 15 hours before being immersed into a mixture of freshly prepared $Zn((NO)_3)_2$ (25 mM) and 2-methylimidazole (50 mM) for 40 minutes. (B)(i – v) Cross sectional scanning electron microscopy (SEM) images of the ZIF-8 film thickness after 1 – 5 ZIF-8 growth cycles. Scale bar, 100 nm.

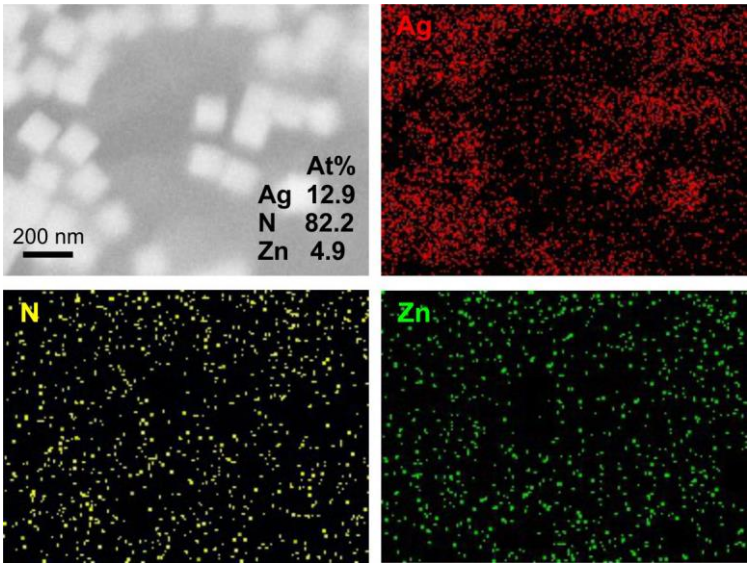

Figure S4. EDS elemental mapping of Ag@ZIF substrate indicating the elemental distribution of Ag (red), N (yellow) and Zn (green).

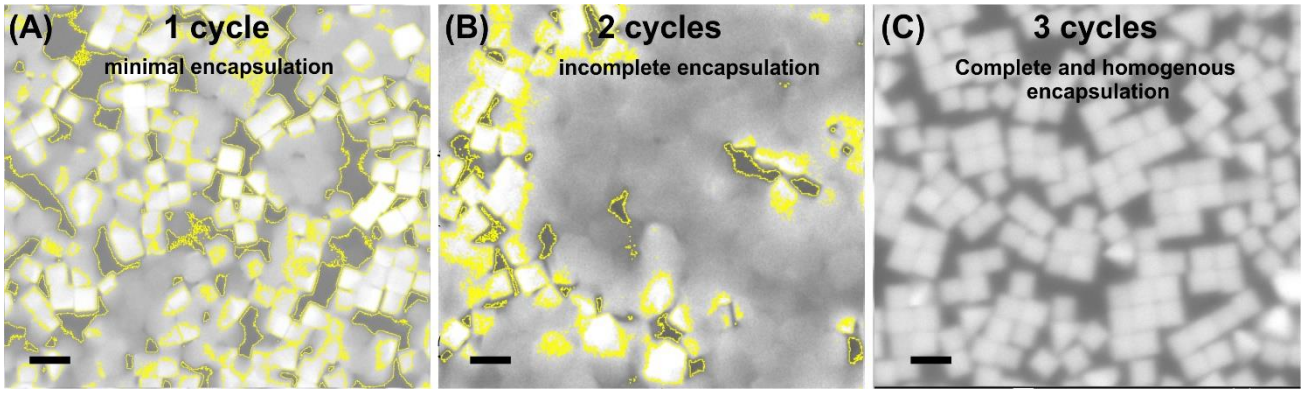

Figure S5. (A-C) SEM images of ZIF-8 film growth after 1 - 3 cycles. Dotted lines show the ZIF-8 film growth (grey) over the nanocubes. The first cycle result in minimal film growth and individual ZIF-8 crystals are observed. Upon additional growth cycle, the film thickens and becomes more continuous but is insufficient to completely encapsulate the Ag nanocubes array. A minimum of 3 cycles is needed to allow complete and homogenous encapsulation of the nanocubes. Yellow lines outline the ZIF-8 film overgrowth on the Ag array. The SEM image appears blur due to the additional layer of ZIF film atop the Ag nanocubes. Scalebar, 200 nm

As the growth cycle is increased from 2 to 3, the coverage increases by 36% to allow complete encapsulation. This enables more gas analyte to accumulate at the nanoparticle surface, which consequently leads to an increase in SERS signal. However, extrapolating from the previous trend of Ag@ZIF-1 to Ag@ZIF-2, this increase in encapsulation is expected to result in linear increase of SERS activity, instead of the sharp and drastic increase in SERS intensity achieved by the Ag@ZIF-3. This therefore evidently demonstrates that the amplified signal of the Ag@ZIF-3 platform is attributed to both the increase in coverage and thickness of the ZIF-8 film, where more gas analyte is allowed to accumulate in the x-, y-, and z- direction respectively.

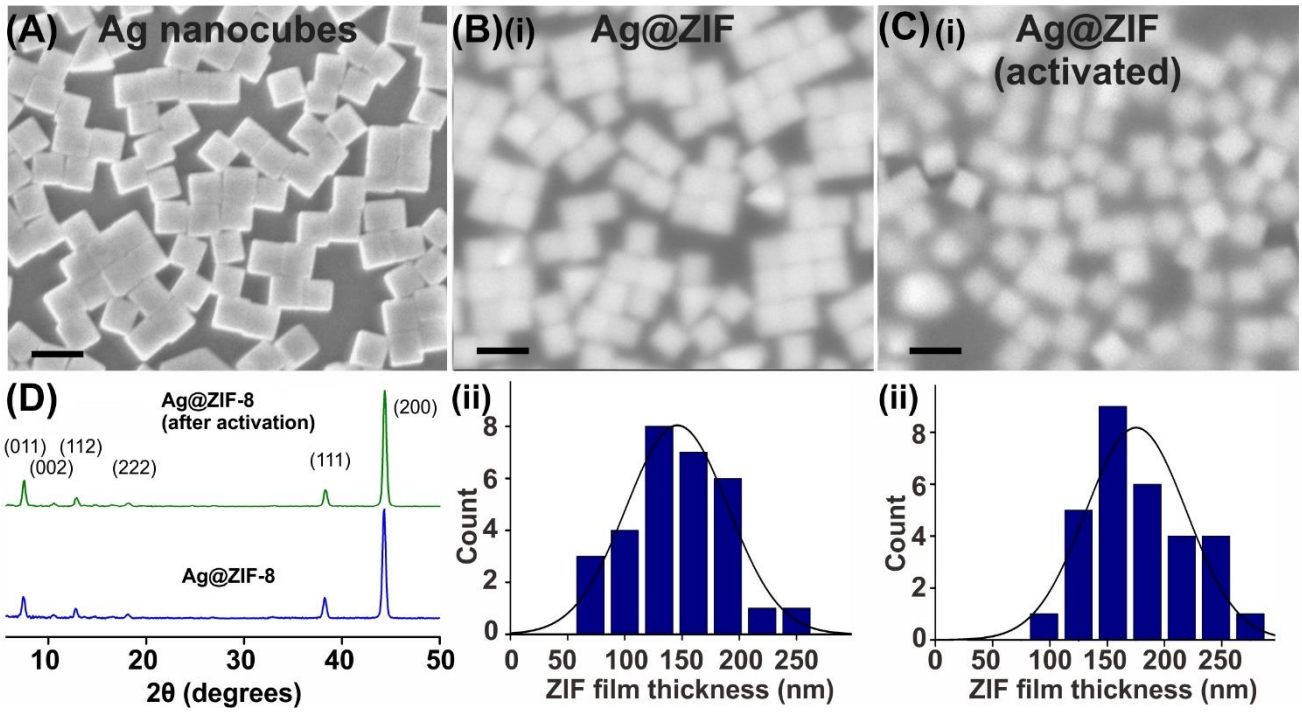

Figure S6. SEM images of Ag nanocubes assembled using surface pressure of 16 mN/ m after (A) functionalization with PFDT, followed by (B) (i) 3 cycles of ZIF-8 and then (C) (i) thermally activated under vacuum at 120ºC for 2 hours. Scale bar, 200 nm. (ii) Thickness distribution of the ZIF film. Thermal stability of ZIF-8 film over Ag nanocubes is reflected by the minimal changes even after activation. (D) XRD spectra before and after activation shows minimal difference.

Ag@ZIF platforms are thermally-activated prior to SERS measurement and this treatment process does not affect Ag@ZIF's structural integrity, as reflected by their similar XRD patterns, film morphology and SERS spectra before and after thermal activation.

Supporting Text S1: Calculation of Analytical Enhancement Factor (AEF)

Calculation of AEF using saturated methylbenzenethiol gas is as follows:

Analytical EF = $[I_{SERS} / I_{Raman}] \times [C_{Raman} / C_{SERS}]$

where C_{SERS} and C_{Raman} are the corresponding concentration measured using Ag@ZIF substrate and normal Raman respectively. I_{SERS} and I_{Raman} are the signals recorded using SERS and normal Raman at their respective concentration per unit time.

C_{SERS} is calculated by manipulating the terms in the ideal gas law:

$$C_{\mathrm{SERS}} = \frac{\mathrm{n}}{\mathrm{V}} = \frac{\mathrm{p}}{\mathrm{RT}} = \frac{108}{8.31 * 298} = 0.0434 \text{ mol/m}^3$$

Where p is the partial pressure (= 108 Pa) at ambient temperature (T = 298 K), and R is the universal gas constant, 8.31 J/Kmol.

C_{Raman} is calculated by dividing the density of 4MBT by its molecular weight:

$$C_{\mathrm{raman}} = \frac{\rho}{\mathrm{MW}} = \frac{1.022 \text{ g/ml}}{124 \text{ g/mol}} = 0.008228 \text{ mol/ml}$$

Hence, using Ag@ZIF substrate formed using surface pressure of 16 mN/ m as an example,

AEF = $[I_{SERS} / I_{Raman}] \times [C_{Raman} / C_{SERS}]$ = (660/ 18) × (8228/ 0.0434)

= 7.10×10^6

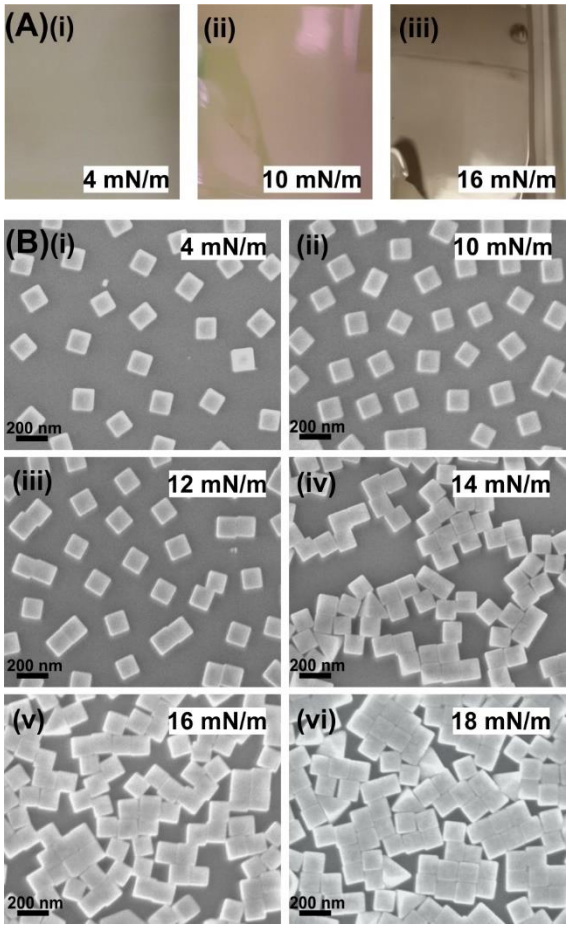

Figure S7. (A) (i-iii) Digital images of the visual changes observed as the compactness of the Ag nanocube array increases from 4, 10, 16 mN/m. (B) (i-vi) SEM images of assembled Ag nanocube array when surface pressure is 4, 10, 12, 14, 16, 18 mN/m respectively.

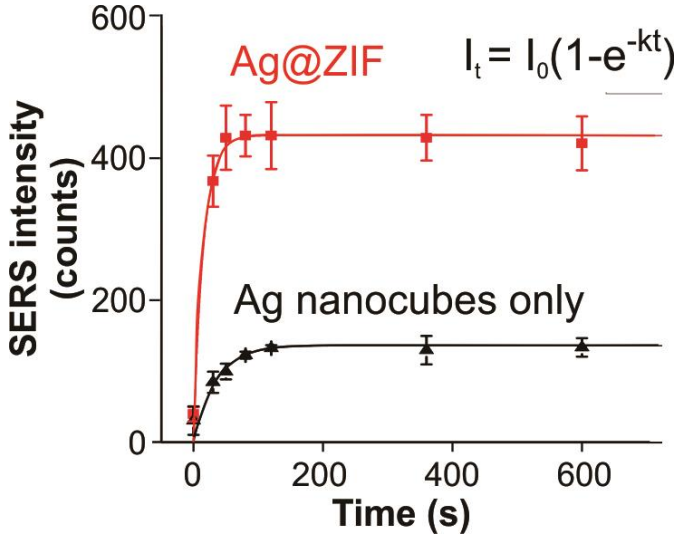

Figure S8. Time-dependent SERS measurement of 4-MBT sorption comparing platforms with (red) and without (black) ZIF film.

Both intensity-time curves can be fitted using a Lagergren pseudo first order adsorption kinetics[5] based on linear driving force model, which is inclined to physisorption of the analyte and follows the equation: $I = I_{max}(1-e^{-kt})$ where I is the time-dependent SERS intensity (in counts) at time t, I_{max} the final equilibrium intensity and k (s^{-1}) gives the pseudo first-order adsorption rate constant. Notably, the rate constant (66 ms^{-1}) is two-fold higher than the control, and the sharp increase in intensity within the first 80 s, further reflects advantage of ZIF-8 in enabling faster capture and preconcentration of the analyte molecules.

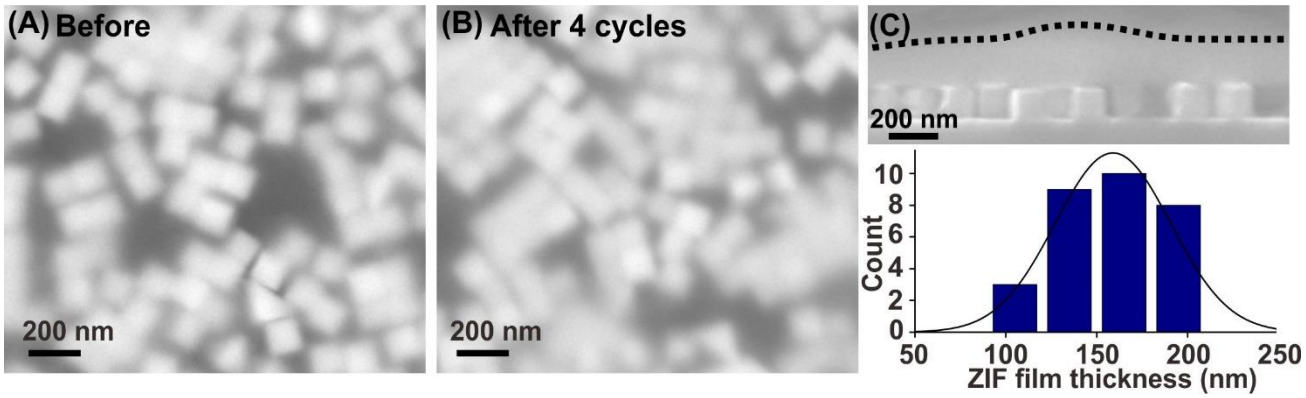

Figure S9. SEM images of Ag@ZIF substrate (A) before and (B) after exposure to toluene for four cycles. ZIF film remains intact even after subjecting the substrate to toluene vapor and vacuum repeatedly. (C) Cross-sectional SEM image (top) and corresponding ZIF-8 film thickness distribution of (B) (bottom). Dotted line denotes the ZIF film layer.

Supporting Text S2: Calculation of vapor concentration from liquid reservoir

The concentration of vapor toluene is varied from 200 to 20000 ppm in the incubation cell by changing the mole fraction of toluene in a toluene-decane mixture based on Raoult's law.[6]

Calculation of concentration of toluene vapor is as follows:

$$\text{Concentration (ppm)} = \frac{n_{toluene}}{n_{total}} \times 10^6$$

Where $n_{toluene}$ and n_{total} is the number of moles of toluene and total number of gas molecules in the closed Raman cell respectively.

Using Raoult's law, which states that the partial pressure of a component in an ideal mixture is equals to the mole fraction of the component in the solution, the resultant partial vapor pressure of toluene in a toluene-decane mixture can be calculated. At temperature 298K, the vapor pressure of toluene and decane is 3760 Pa and 190 Pa respectively. By changing the mole ratio of decane/toluene, different concentration of toluene vapor can be obtained. The table below shows the volumes used for different vapor concentration.

Volume of Toluene (µl)	Volume of decane (µl)	Mole fraction of toluene	Partial Vapor Pressure of toluene (Pa)	Partial Vapor Pressure of decane (Pa)	Concentration of toluene (ppm)
1000	2000	0.47834	1799	99	17424
250	1000	0.31435	1182	131	11516
266	2235	0.17916	674	156	6594
35	1000	0.06031	227	179	2229
53	4950	0.01927	72	187	713
5	938	0.00968	36	189	358
3	1000	0.00547	21	190	203

For example, to achieve a vapor concentration of 17424 ppm, 1000 µl of toluene is mixed with 2000 µl of decane. Also given that the density of toluene and decane is 0.8669 g/ ml and 0.7300 g/ ml respectively,

$$\text{Mole fraction} = \frac{V_1\rho_1/Mr_1}{V_1\rho_1/Mr_1 + V_2\rho_2/Mr_2}$$

$$= \frac{0.1 \times 0.8669/92.14}{0.1 \times 0.8669/92.14 + 0.2 \times 0.73/142.29} = 0.47834$$

Where V is the volume of component used in ml, ρ is the density in g/ml and Mr is the molecular weight in g/mol. Component 1 represents toluene while component 2 represents decane.

$$\text{Vapor pressure of toluene} = \text{mole fraction in solution} \times \text{vapor pressure}$$

$$= 0.47834 \times 3760 = 1799 \text{ Pa}$$

$$\text{Vapor Concentration (ppm)} = \frac{1799}{1799+(1-0.47834)\times 190+101325} \times 10^6 = 17424$$

Reports have found that there is a risk of central nervous system (CNS) depression, the inhibition of brain activity, upon the first few minutes of toluene vapor exposure with concentration of 10000 – 30000 ppm, and possibly death for longer exposure times.[7] Even at lower concentrations, the acute effects include reaction time impairment and incoordination, and is especially dangerous for people working in high-hazard industries, thus emphasizing the necessity for rapid and timely detection of toluene leakages.

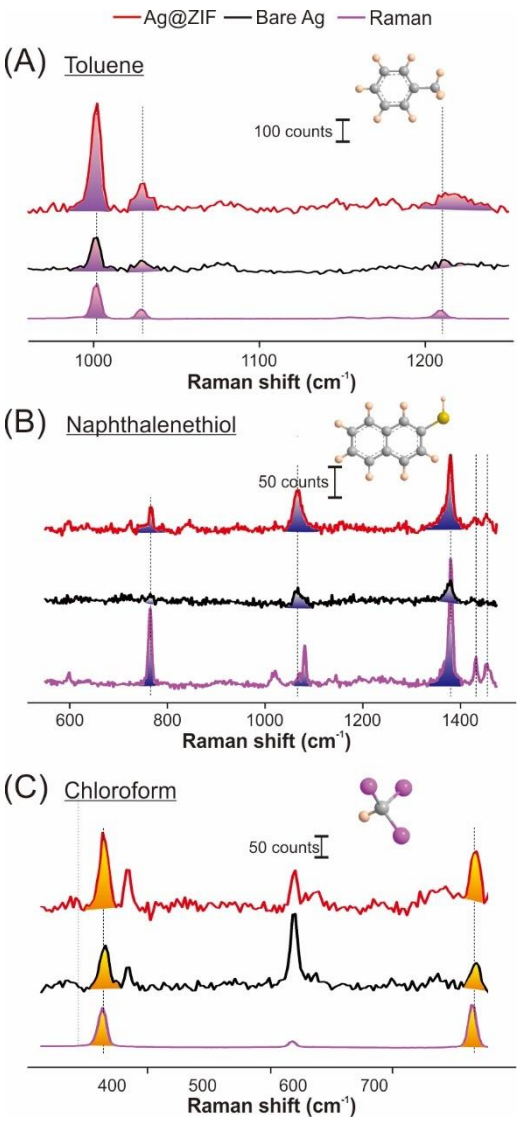

Figure S10. (A – C) SERS spectrum comparing detection of 2-naphthalenethiol, chloroform and toluene in gaseous phase using Ag@ZIF substrate (red) and Ag only (black). Raman spectra (pink) of the liquid solvent is added for reference. Inset shows the molecular structure of each VOC. Carbon, Hydrogen, Sulphur and Chlorine atoms are represented by grey, beige, yellow and magenta spheres respectively.

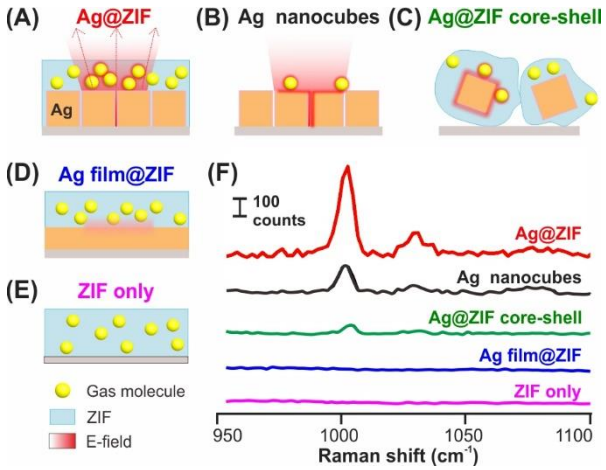

Figure S11. Demonstration on the superior SERS performance of Ag@ZIF. (A) Scheme of the Ag@ZIF platform with other control platforms such as (B) Ag nanocubes only, (C) Ag@ZIF core-shell particles, (D) Ag film@ZIF and (E) neat ZIF platform, and (F) comparison of their SERS activity.

We further compare the SERS performance of our Ag@ZIF plasmonic nose across other control platforms to highlight the importance of each individual components in our combinative approach. These control platforms include bare Ag nanocubes (absence of ZIF), core-shell Ag@ZIF dispersed onto a Si substrate (absence of intense plasmonic coupling), Ag film@ZIF and ZIF only platforms (Figure S11, S12). Generally, Ag@ZIF ensemble clearly outperforms all other platforms, achieving > 2-fold and 6-fold higher SERS sensitivity than Ag nanocubes only and Ag@ZIF core shell, respectively. The superior performance of our Ag@ZIF platform stems from its ability to concentrate both molecules and EM field cumulatively for better SERS enhancement compared to controls without ZIF or assembled arrays. We also note that control Ag film@ZIF and ZIF only platforms exhibit featureless spectra, again accentuating the need for high quality plasmonic crystal for sensitive SERS read-out. Our findings collectively highlight that MOF-enabled molecular preconcentration and intense EM field generated by extensive plasmonic coupling between Ag nanocubes are the key to ultrasensitive and swift vapor/gas detection. These benefits are highly sought after to ensure timely response necessary to protect the safety of the public in event of potential toxic gas leakage and/or air pollution from anthropogenic or natural sources.

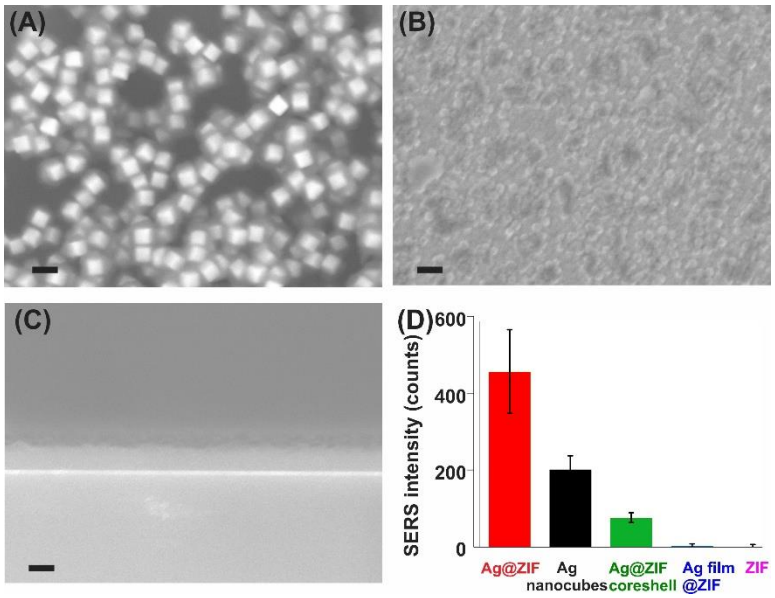

Figure S12. SEM images of the control platforms; (A) Ag@ZIF core-shell, (B) Ag film@ZIF and (C) ZIF film (cross-sectional view) only. Scale bar, 200 nm. Comparison of the SERS performance of different platforms. The SERS intensities are obtained from the 1002 cm^{-1} band of toluene.

References

1. M. Mulvihill, A. Tao, K. Benjauthrit, J. Arnold and P. Yang, *Angew. Chem. Int. Ed.*, 2008, **47**, 6456-6460.

2. G. Lu and J. T. Hupp, *J. Am. Chem. Soc.*, 2010, **132**, 7832-7833.

3. Y. H. Lee, H. Chen, Q.-H. Xu and J. Wang, *J. Phys. Chem. C*, 2011, **115**, 7997-8004.

4. H. K. Lee, Y. H. Lee, I. Y. Phang, J. Q. Wei, Y. E. Miao, T. X. Liu and X. Y. Ling, *Angew. Chem. Int. Ed.*, 2014, **53**, 5054-5058.

5. S. Lagergren, *Kungliga Svenska Vetenskapsakademiens. Handlingar*, 1898, **24**, 1 - 39.

6. R. Kodiyath, S. T. Malak, Z. A. Combs, T. Koenig, M. A. Mahmoud, M. A. El-Sayed and V. V. Tsukruk, *J. Mater. Chem. A*, 2013, **1**, 2777-2788.

7. D. O. B. Zenz C., Horvath EP Jr., *Occupational Medicine*, MO: Mosby-Year Book, Inc., St. Louis, 3 edn., 1994.